Supplemental Data

Supplemental Results

Cholestenoic Acids and their Precursors are Present in Mouse Brain. Earlier studies have shown that rat fetal neurons can synthesize 3β-HCA from 26-HC and that rat astrocytes can synthesize this acid, as well as 3β,7α-diHCA and 7αH,3O-CA from 26-HC (1). In addition we have identified 26-HC and its metabolite 7α,26-diHC in newborn mouse brain and in adult rat brain, respectively (2,3). Thus, to provide further evidence for the hypothesis that cholestenoic acids are synthesised in the CNS we analysed the sterol content of adult mouse brain and found low levels of 26-HC (0.1 - 1 ng/mg), 7α,26-diHC plus 7α,26-diHCO (<0.03 ng/mg) and 3β-HCA (<0.01 ng/mg) (Table S4). These data matches that from embryonic mouse and adult human brain which shows similarly low levels of 26-HC and the down-stream metabolite 7α,26-diHC (4,5).

Figure S1

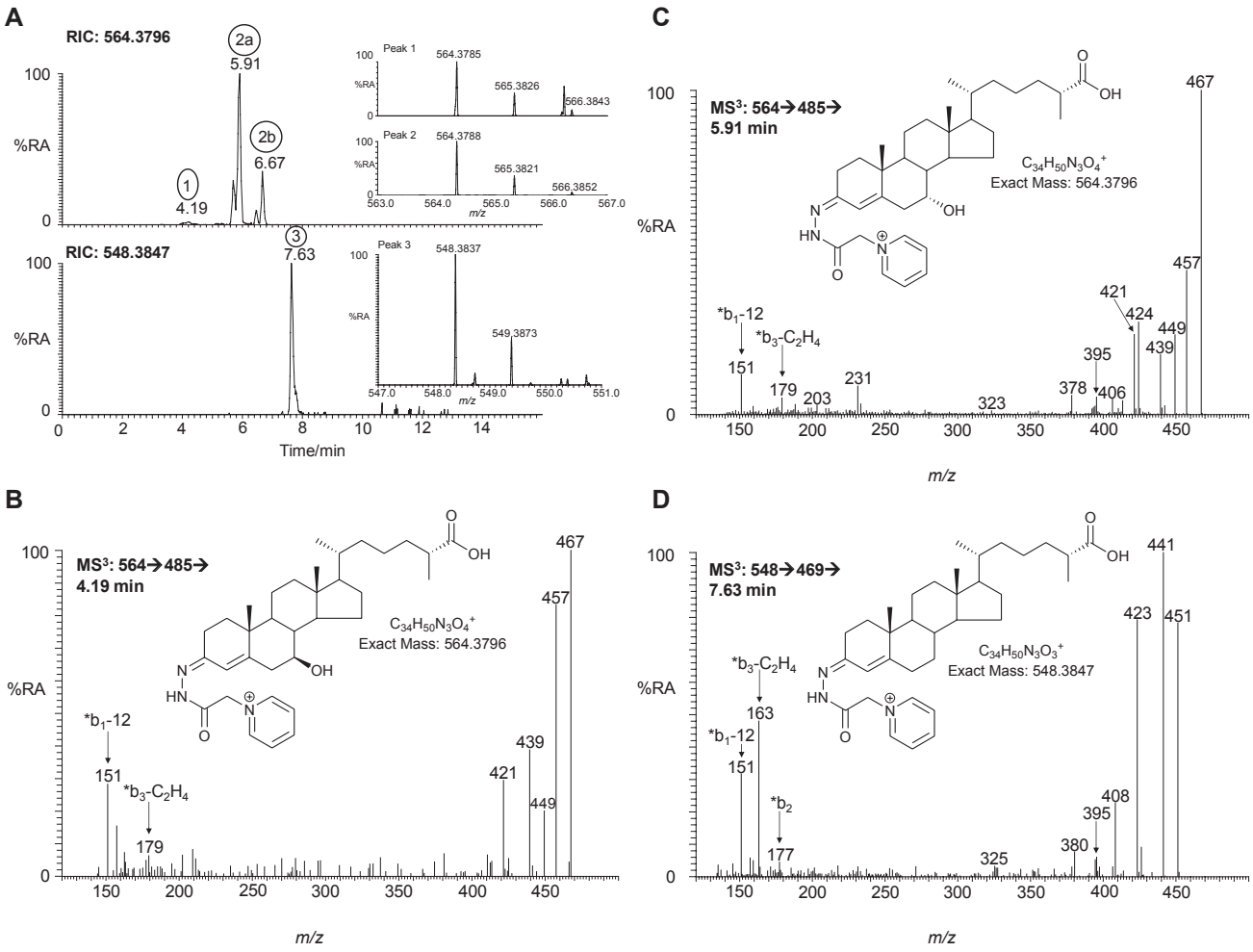

Figure S1. Identification of cholestenoic acids in human CSF. (A) LC-ESI-MS reconstructed ion chromatograms (RICs ± 5 ppm) of the cholestenoic acids: 3β,7β-diHCA peak 1, 7αH,3O-CA/3β,7α-diHCA peaks 2, and 3β-HCA peak 3. The insets show the molecular ions corresponding to the peaks 1, 2a and 3. Sterols were extracted from CSF in ethanol, fractionated according to hydrophobicity by SPE and "charge-tagged" with the GP reagent to give maximum sensitivity upon LC-ESI-MS analysis. The first step of the charge-tagging process involves oxidation of 3β-hydroxy-5-ene groups to 3-oxo-4-enes by cholesterol oxidase from *Streptomyces sp*. Endogenous 3-oxo-4-ene containing compound are differentiated from those derived from 3β-hydroxy-5-enes by repeating the charge-tagging reactions, but in the absence of oxidizing enzyme. The charge-tagging process introduces *syn* and *anti* conformers (peaks a and b) which may or may not be resolved. (B-D) LC-ESI-MS^3 spectra of the three acids in A. Structures of the precursor ions fragmented by MS^3 ($[M]^+ \rightarrow [M-79]^+ \rightarrow$) are shown. Fragmentation nomenclature has been described previously (3,6,7). The retention times and MS^3 spectra are identical to those of authentic standards. Spectra were recorded on the LTQ-Orbitrap. In this work we have adopted the sterol nomenclature recommended by the lipid maps consortium, where 26-hydroxycholesterol, 26-HC, refers to cholest-(25R)-5-en-3β,26-diol, and similarly, carboxylic acids which introduce 25R stereochemistry to the side-chain are at C-26 (8).

Figure S2

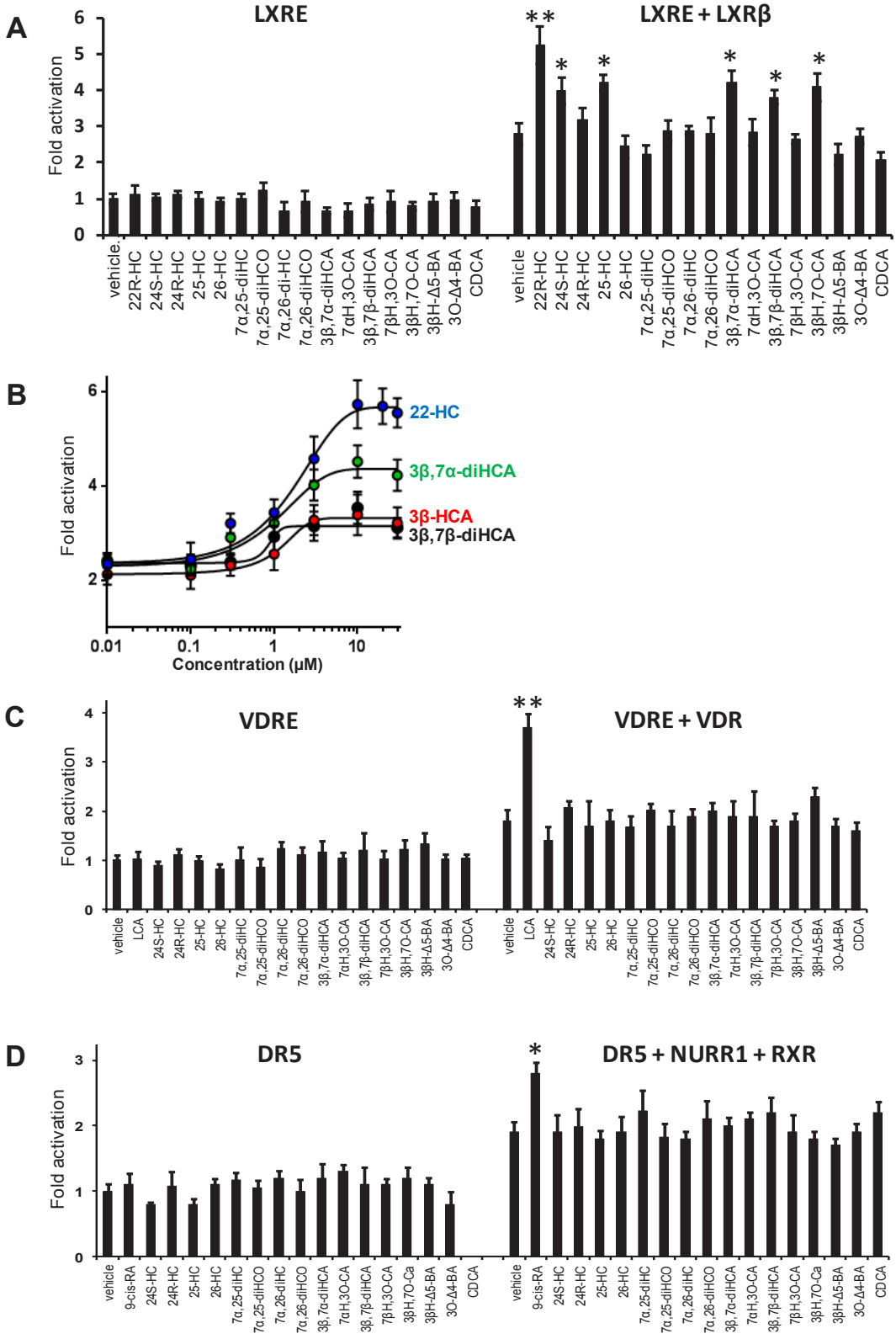
A
LXRE
LXRE + LXRβ
Fold activation
vehicle
22R-HC
24S-HC
24R-HC
25-HC
26-HC
7α,25-diHC
7α,25-diHCO
7α,26-di-HC
7α,26-diHCO
3β,7α-diHCA
7αH,3O-CA
3β,7β-diHCA
7βH,3O-CA
3βH,7O-CA
3βH-Δ5-BA
3O-Δ4-BA
CDCA
B
Fold activation
22-HC
3β,7α-diHCA
3β-HCA
3β,7β-diHCA
0.01
0.1
1
10
Concentration (μM)
C
VDRE
VDRE + VDR
Fold activation
vehicle
LCA
24S-HC
24R-HC
25-HC
26-HC
7α,25-diHC
7α,25-diHCO
7α,26-diHC
7α,26-diHCO
3β,7α-diHCA
7αH,3O-CA
3β,7β-diHCA
7βH,3O-CA
3βH,7O-CA
3βH-Δ5-BA
3O-Δ4-BA
CDCA
D
DR5
DR5 + NURR1 + RXR
Fold activation
vehicle
9-cis-RA
24S-HC
24R-HC
25-HC
26-HC
7α,25-diHC
7α,25-diHCO
7α,26-diHC
7α,26-diHCO
3β,7α-diHCA
7αH,3O-CA
3β,7β-diHCA
7βH,3O-CA
3βH,7O-Ca
3βH-Δ5-BA
3O-Δ4-BA
CDCA

Figure S2. Analysis of the nuclear receptor activational capacity of oxysterols and cholestenoic acids. (A) Analysis of luciferase activity in SN4741 cells transfected with an LXR responsive luciferase reporter construct (LXRE) and LXRβ and stimulated for 24 h with 22R-HC (10 μM), a known LXRβ ligand, or the compounds indicated (10 μM). (B) Dose response curves for the activational capacity of cholestenoic acids and 22R-HC on LXRβ (n = 3). Concentration is plotted on a log scale. EC_{50} values: 22R-HC: 1.91 μM; 3β,7α-diHCA: 1.43 μM; 3β,7β-diHCA: 0.92 μM; 3β-HCA: 1.73 μM; efficacy values: 22R-HC: 1; 3β,7α-diHCA: 0.61; 3β,7β-diHCA: 0.24; 3β-HCA: 0.31. Similar experiments were performed with cells transfected with (C) VDRE and VDR; and (D) DR5 and NURR1. LCA is a known VDR ligand. 9-cis-RA is a known RXR ligand. RXR is the heterodimer partner of NURR1. Other compounds tested were 24S-HC; 24R-HC; 25-HC; 26-HC; 7α,25-diHC; 7α,25-diHCO; 7α,26-diHC; 7α,26-diHCO; 3β,7α-diHCA; 7αH,3O-CA; 3β,7β-diHCA; 7βH,3O-CA; 3βH,7O-CA; 3βH-Δ^5-BA; 3O-Δ^4-BA; CDCA. The firefly luciferase activity was normalized to Renilla luciferase activity, and the values are expressed as fold activation over the normalized basal response element-luciferase activity set to 1. Data in A, C, D are means ± SEM (n = 3), *, $P < 0.05$; **, $P < 0.01$, by Mann-Whitney test, compared to vehicle treatment.

Figure S3

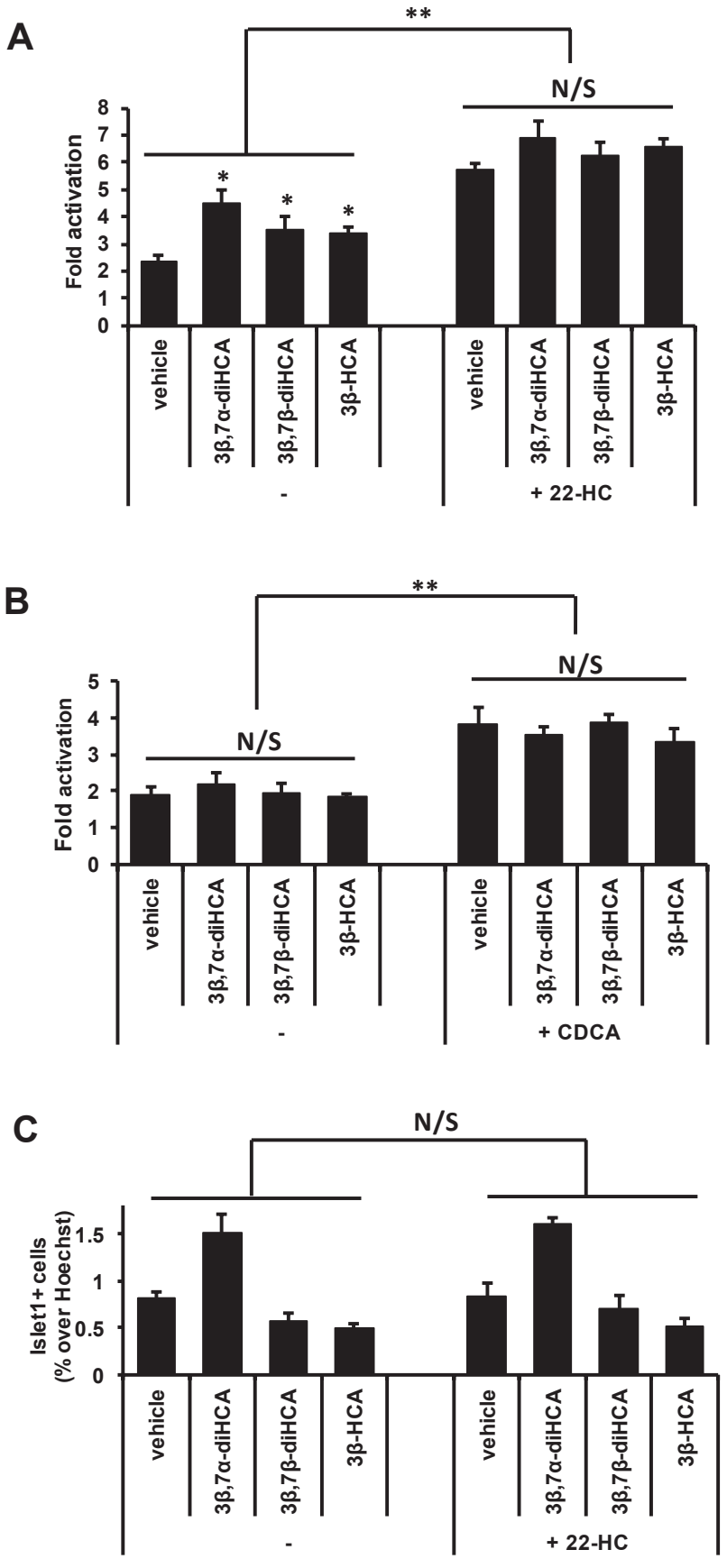
A
**
N/S
Fold activation
8
7
6
5
4
3
2
1
0
*
*
*
vehicle
3β,7α-diHCA
3β,7β-diHCA
3β-HCA
vehicle
3β,7α-diHCA
3β,7β-diHCA
3β-HCA
-
+ 22-HC
B
**
N/S
N/S
Fold activation
5
4
3
2
1
0
vehicle
3β,7α-diHCA
3β,7β-diHCA
3β-HCA
vehicle
3β,7α-diHCA
3β,7β-diHCA
3β-HCA
-
+ CDCA
C
N/S
Islet1+ cells
(% over Hoechst)
1.5
1
0.5
0
vehicle
3β,7α-diHCA
3β,7β-diHCA
3β-HCA
vehicle
3β,7α-diHCA
3β,7β-diHCA
3β-HCA
-
+ 22-HC

Figure S3. Effects of cholestenoic acids in combination with other nuclear receptor agonists. (A) LXRβ activational capacity of 3β,7α-diHCA, 3β,7β-diHCA and 3β-HCA (10 μM) in combination with 22R-HC (10 μM). (B) Similar experiments performed with FXR, the three cholestenoic acids and CDCA (10 μM). The experiments in (A) and (B) were performed otherwise as in Figure S2. (C) Quantification of Islet1+ cells in mouse E11.5 brain primary cultures treated with 10 μM 3β,7α-diHCA, 2 μM 3β,7β-diHCA or 2 μM 3β-HCA in combination with 22R-HC. Data are means ± SEM (n = 3), **, $P < 0.01$, by Mann-Whitney test, as indicated.

Figure S4

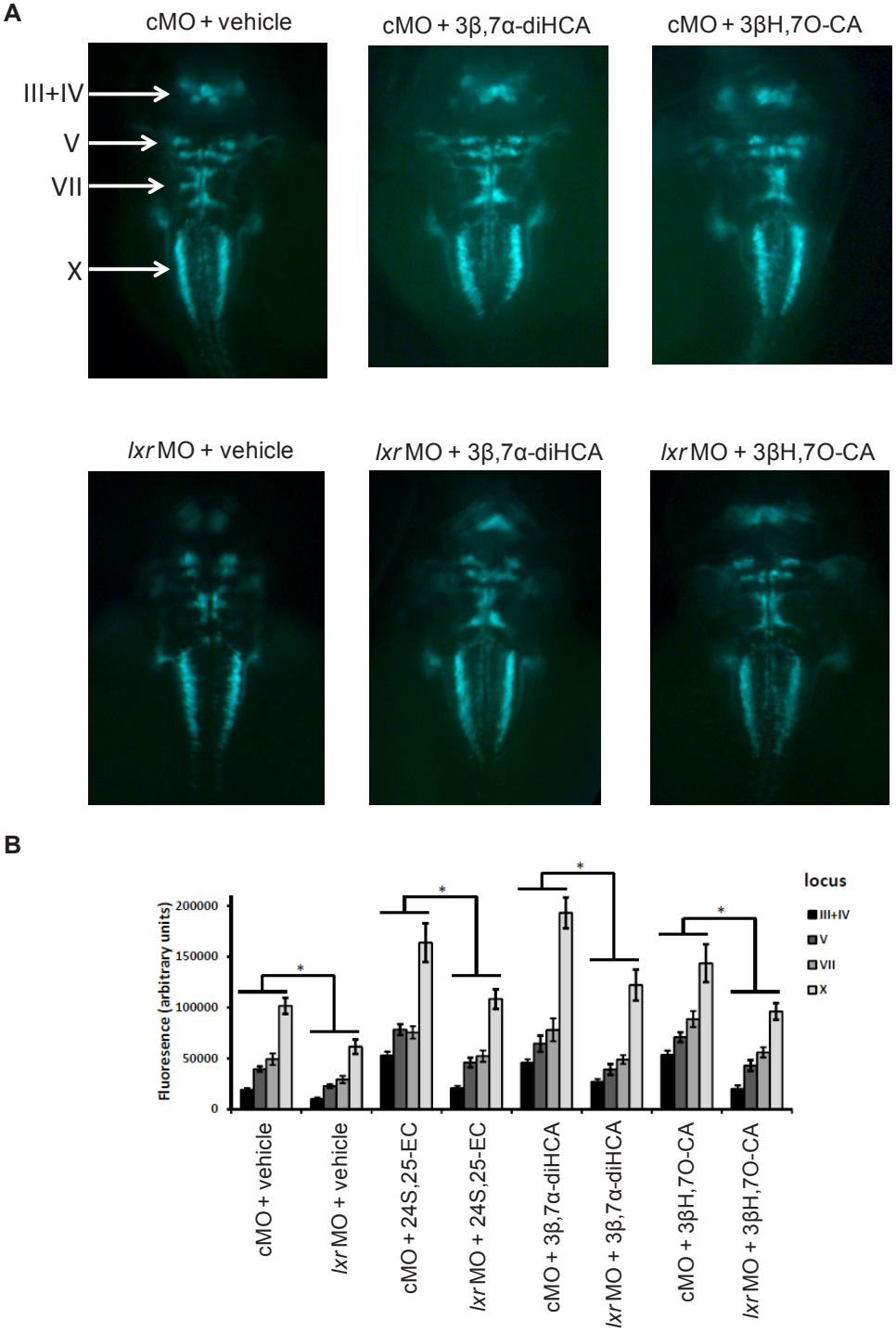

Figure S4. 3β,7α-diHCA and 3βH,7O-CA require LXR for expression of motor neuron markers in zebrafish. (A) *lxr* morpholinos (*lxr* MO) abolished the effects of the two acids on Islet-1 expression. Control scrambled MO (cMO, upper panel) or *lxr* MO (lower panel) injected Tg[*Isl1*:GFP] embryos were incubated with 10 μM test compound or vehicle added to medium, and the medium was replaced every 12 h with fresh solution (containing test compound or vehicle). Immunocytochemistry was performed using an anti-GFP antibody. Dorsal views of the head/upper back region of embryos treated with vehicle, 3β,7α-diHCA or 3βH,7O-CA are shown. Arrows indicate loci III, IV, V, VII and X. (B) Quantification of Islet-GFP signal intensity in the different cranial nerves/loci. 24,25-EC was used as a positive control. Data are means ± SEM (n = 4), *, $P < 0.05$, by Mann-Whitney test, compared to each respective cMO group.

Figure S5

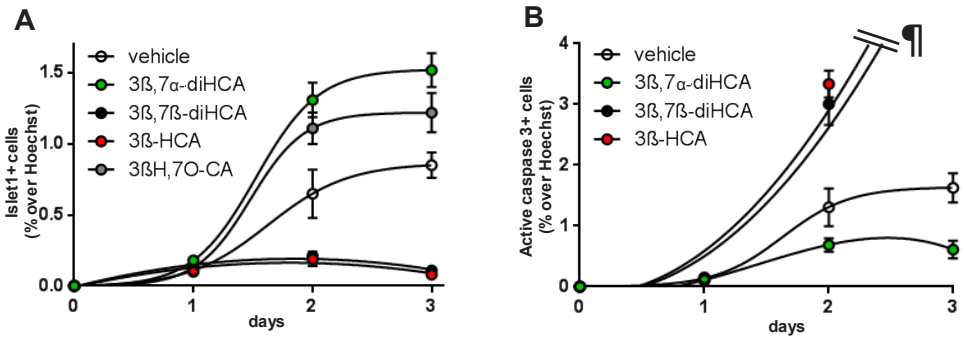

Figure S5. Time course analysis and quantification of the number of Islet1+ and active caspase 3+ cells in mouse E11.5 brain primary cultures. Time course analysis for the quantification of (A) Islet1+ cells and (B) active caspase 3+ cells in mouse E11.5 brain primary cultures treated with 3β,7α-diHCA, 3β,7β-diHCA, 3β-HCA or 3βH,7O-CA. The symbol ¶ indicates very high cell death in the cultures. Data are means ± SEM (n = 3).

Figure S6

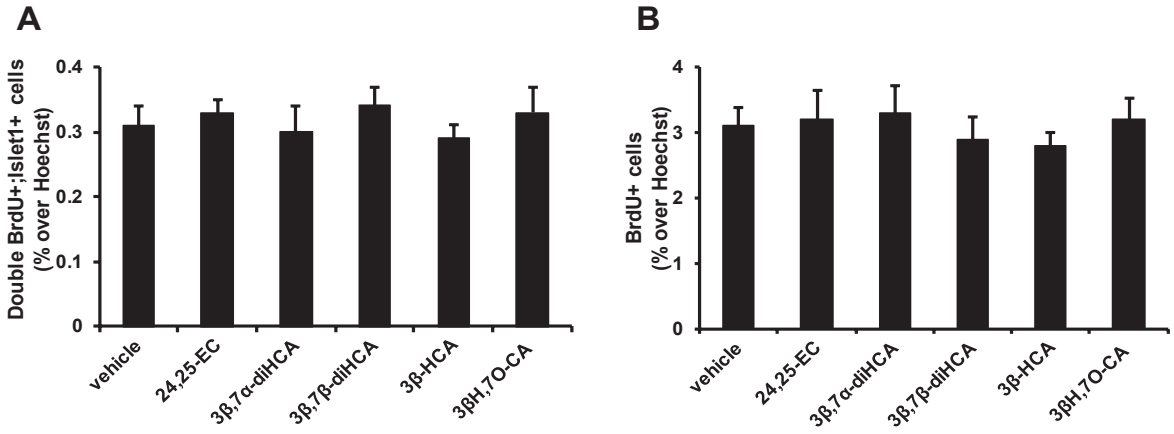

Figure S6. No effect of 24,25-EC, 3β,7α-diHCA, 3β,7β-diHCA, 3β-HCA and 3βH,7O-CA on motor neuron neurogenesis or on proliferation. (A) Neurogenesis was examined in BrdU pulse-chase experiments, where neuronal progenitors in primary cultures were labelled with a pulse of BrdU at the beginning of the experiment and then examined for their differentiation into motor neurons, as assessed by the acquisition of Islet-1 expression. None of the compounds studied affected the number of double BrdU+;Islet+ cells, indicating that they do not promote motor neuron neurogenesis. (B) None of the compounds studied affected the total number of BrdU+ cells in the cultures, indicating that they do not modulate proliferation.

Figure S7

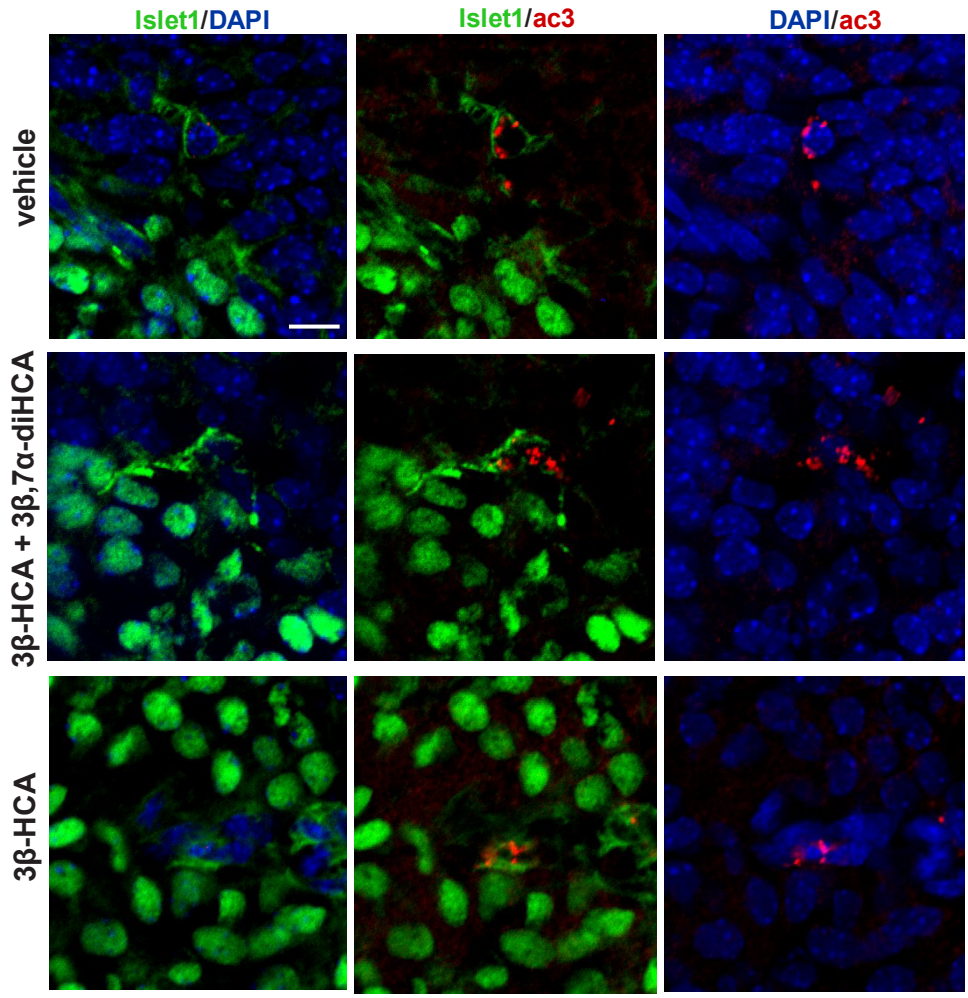

Figure S7. Morphological appearance of cells identified as double-positive Islet1+;ac3+ cells in vivo. The cholestenoic acids 3β,7α-diHCA and 3β-HCA, or 3β-HCA were injected into the cerebral aqueduct of E11.5 mice in utero and coronal brain sections were analyzed at E13.5 for double-positive Islet1+;ac3+ cells. A very limited number of oculomotor neurons were undergoing apoptosis in vivo. Representative images of Islet1+/DAPI, Islet1+/ac3+, and DAPI/ac3+ stained cells are shown. Scale bar: 5 μm.

Table S1. Oxysterols and Cholestenoic Acids in Human CSF

Oxysterols and cholestenoic acids identified by LC-ESI-MS^n in CSF following SPE and charge-tagging with GP-hydrazine. In the absence of authentic standards presumptive identifications based on exact mass, MS^n spectra and retention time are given. A pooled sample from 15 control subjects (black ‡) was analysed. Additionally, selected oxysterols and cholestenoic acids were analysed from 18 individual control subjects (blue †). CSF from three SPG5 patients (purple*), and two health carriers, heterozygotes, with a single mutation in *CYP7B1*, (green•) was also analysed.

After cholesterol oxidase and GP-tagging			Originating structure					Note
Mass	Formula	Sterol Systematic name	Sterol Systematic name (Common name, abbreviation)	RT	RRT	AS	Mean concentration ng/mL ± SEM	
522.3326	$C_{31}H_{44}N_3O_4^+$	7α-Hydroxy-3-oxochol-4-en-24-oic acid 3-GP	7α-Hydroxy-3-oxochol-4-en-24-oic acid (7αH,3O-Δ^4-BA)	2.06	0.34	Yes	0.507±0.088‡ 0.423±0.128• 0.058±0.026*	1,2,3
534.3690	$C_{33}H_{48}N_3O_3^+$	7α-Hydroxy-26-nor-cholest-4-ene-3,**24**-dione 3-GP	7α-Hydroxy-26-nor-cholest-4-ene-3,**24**-dione	4.86	0.82	No	0.712±0.093‡ 0.140±0.038• 0.022±0.022*	1,2,3, 4
534.4054	$C_{34}H_{52}N_3O_2^+$	24S-Hydroxycholest-4-en-3-one 3-GP	Cholest-5-ene-3β,24S-diol (24S-Hydroxycholesterol, 24S-HC)	7.43	1.26	Yes	0.075±0.003‡ 0.032±0.010• 0.018±0.006*	5,6
534.4054	$C_{34}H_{52}N_3O_2^+$	25-Hydroxycholest-4-en-3-one 3-GP	Cholest-5-ene-3β,25-diol (25-Hydroxycholesterol, 25-HC)	7.64	1.30	Yes	0.026±0.003‡ 0.030±0.005† 0.041±0.018• 0.166±0.048*	3,5,6, 7
534.4054	$C_{34}H_{52}N_3O_2^+$	26-Hydroxycholest-4-en-3-one 3-GP	Cholest-5-ene-3β,26-diol (26-Hydroxycholesterol, 26-HC)	7.99	1.36	Yes	0.146±0.003‡ 0.100±0.007† 0.215±0.032• 0.915±0.224*	3,5,6, 7
534.4054	$C_{34}H_{52}N_3O_2^+$	7β-Hydroxycholest-4-en-3-one 3-GP	Cholest-5-ene-3β,7β-diol (7β-Hydroxycholesterol, 7β-HC)	9.68	1.62	Yes	0.032±0.027‡ 0.138±0.060• 0.079±0.022*	3,5,6
534.4054	$C_{34}H_{52}N_3O_2^+$	7α-Hydroxycholest-4-en-3-one 3-GP	Cholest-5-ene-3β,7α-diol (7α-Hydroxycholesterol, 7α-HC)	10.20	1.72	Yes	0.026±0.017‡ 0.190±0.091• 0.122±0.034*	3,5,6
534.4054	$C_{34}H_{52}N_3O_2^+$	6-Hydroxycholest-4-en-3-one 3-GP	Cholest-4-ene-3β,6-diol or Cholest-5-ene-3β,6-diol	10.52	1.77	Yes	0.149±00.042‡ 1.419±1.174•	3,5,6, 8

			(6-Hydroxycholesterol, 6-HC)				0.235±0.138*	
546.3690	$C_{34}H_{48}N_3O_3^+$	3-Oxocholesta-4,6-dien-26-oic acid 3-GP	3-Oxocholesta-4,6-dien-26-oic acid	7.28	1.23	Yes	2.047±0.312‡ 1.546±0.110† 1.182±0.319• 0.159±0.111*	1,3,5,7,9
546.3690	$C_{34}H_{48}N_3O_3^+$	3-Oxocholesta-4,6-dien-26-oic acid 3-GP	3β-Hydroxycholesta-5,7-dien-26-oic acid	7.28	1.23	No	0.467±0.015‡ 0.079±0.023† 0.213±0.092• 0.079±0.045*	1,2,3,7,10
548.3847	$C_{34}H_{50}N_3O_3^+$	3-Oxocholest-4-en-26-oic acid 3-GP	3β-Hydroxycholest-5-en-26-oic acid (3β-HCA)	7.63	1.30	Yes	1.458±0.095‡ 0.959±0.098† 2.749±0.098• 20.145±2.756*	1,3,5,7
550.4003	$C_{34}H_{52}N_3O_3^+$	7α,25-Dihydroxycholest-4-en-3-one 3-GP	7α,25-Dihydroxycholest-4-en-3-one (7α,25-diHCO)	5.71	0.96	Yes	0.039±0.001‡ 0.039±0.002• ND*	1,3,5,11
550.4003	$C_{34}H_{52}N_3O_3^+$	7α,25-Dihydroxycholest-4-en-3-one 3-GP	Cholest-5-ene-3β,7α,25-triol (7α,25-Dihydroxycholesterol, 7α,25-diHC)	5.71	0.96	Yes	0.028±0.003‡ 0.045±0.034• 0.015±0.015*	1,3,5,11
550.4003	$C_{34}H_{52}N_3O_3^+$	7α,26-Dihydroxycholest-4-en-3-one 3-GP	7α,26-Dihydroxycholest-4-en-3-one (7α,26-diHCO)	6.23	1.05	Yes	0.045±0.002‡ 0.055±0.018• ND*	1,3,5
550.4003	$C_{34}H_{52}N_3O_3^+$	7α,26-Dihydroxycholest-4-en-3-one 3-GP	Cholest-5-ene-3β,7α,26-triol (7α,26-Dihydroxycholesterol, 7α,26-diHC)	6.23	1.05	Yes	0.028±0.003‡ 0.043±0.010• 0.005±0.003*	1,3,5
562.3639	$C_{34}H_{48}N_3O_4^+$	**24**-Hydroxy-3-oxocholesta-4,6-dien-26-oic acid 3-GP	**24**-Hydroxy-3-oxocholesta-4,6-dien-26-oic acid	4.05	0.68	No	0.160±0.035‡ 0.313±0.067• 0.031±0.031*	1,2,3,12
562.3639	$C_{34}H_{48}N_3O_4^+$	**25**-Hydroxy-3-oxocholesta-4,6-dien-26-oic acid 3-GP	**25**-Hydroxy-3-oxocholesta-4,6-dien-26-oic acid	5.18	0.86	No	0.054±0.013‡ ND• ND*	1,2,3,13
564.3796	$C_{34}H_{50}N_3O_4^+$	7β-Hydroxy-3-oxocholest-4-en-26-oic acid 3-GP	3β,7β-Dihydroxycholest-5-en-26-oic acid (3β,7β-diHCA)	4.18	0.71	Yes	0.555±0.027‡ 0.403±0.044† 0.402±0.100• 0.054±0.043*	1,3,5,7
564.3796	$C_{34}H_{50}N_3O_4^+$	**22**,**25**-Dihydroxycholest-4-en-3,**24**-dione 3-GP	3β,**22**,**25**-Trihydroxycholest-5-en-**24**-one	5.12	0.87	No	0.269±0.033‡ 0.211±0.053•	1,2,3,14

							0.223±0.044*	
564.3796	$C_{34}H_{50}N_3O_4^+$	7α-Hydroxy-3-oxocholest-4-en-26-oic acid 3-GP	7α-Hydroxy-3-oxocholest-4-en-26-oic acid (7αH,3O-CA)	5.91	1.00	Yes	19.476±2.490‡ 17.396±1.090† 20.156±7.774• 2.492±1.316*	1,3,5, 7,9
564.3796	$C_{34}H_{50}N_3O_4^+$	7α-Hydroxy-3-oxocholest-4-en-26-oic acid 3-GP	3β,7α-Dihydroxycholest-5-en-26-oic acid (3β,7α-diHCA)	5.91	1.00	Yes	5.884±0.460‡ 2.121±0.388† 4.547±1.941• 0.472±0.438*	1,3,5, 7,10
566.3952	$C_{34}H_{52}N_3O_4^+$	7α,**24**(or**26**),25-Trihydroxycholest-4-en-3-one 3-GP	7α,**24**(or**26**),25-Trihydroxycholest-4-en-3-one	2.63	0.45	No	0.261±0.010‡ 0.089±0.089• ND*	1,2,3, 15
578.3589	$C_{34}H_{48}N_3O_5$+	7α-Hydroxy-3,**24**-*bis*oxocholest-4-en-26-oic acid 3-GP	7α-Hydroxy-3,**24**-*bis*oxocholest-4-en-26-oic acid	2.34	0.39	No	0.200±0.029‡ 0.233±0.054• ND*	1,2,3, 16
580.3745	$C_{34}H_{50}N_3O_5^+$	7α,**24**-Dihydroxy-3-oxocholest-4-en-26-oic acid 3-GP	7α,**24**-Dihydroxy-3-oxocholest-4-en-26-oic acid	2.66	0.44	No	3.506±0.540‡ 4.514±1.126• 0.603±0.380*	1,2,3, 17
580.3745	$C_{34}H_{50}N_3O_5^+$	7α,**25**-Dihydroxy-3-oxocholest-4-en-26-oic acid 3-GP	7α,**25**-Dihydroxy-3-oxocholest-4-en-26-oic acid	3.64	0.61	No	1.071±0.270‡ 1.204±0.665• 0.191±0.157*	1,2,3, 18
596.3694	$C_{34}H_{50}N_3O_6^+$	Trihydroxy-3-oxocholest-4-en-26-oic acid 3-GP	Trihydroxy-3-oxocholest-4-en-26-oic acid	2.15	0.27	No	0.108±0.019‡ 0.036±0.007• 0.059±0.023*	1,2,3, 19

RT = Retention time/min, RRT = Retention time relative to 7α-hydroxy-3-oxocholest-4-en-26-oic acid, AS = Authentic standard, SEM = Standard error of the mean of three technical replicates of the pooled control sample, of 18 individual control samples, of three SPG5 patients and of two healthy heterozygote carriers, NM = not measured, ND = not detected. In some cases the exact location of side-chain oxo and hydroxy groups is equivocal in which case the most likely location is shown in **bold**.

1. Quantitative estimate based on [$^2H_6$]cholest-5-ene-3β,24(R/S)-diol internal standard.
2. Identification based on exact mass and MS^n spectra.
3. Quantitative measurements based on GP-tagged 3-oxo-4-ene compounds giving similar ESI-MS response (9).
4. 26-Nor-sterol is a likely decomposition product of a 24-oxo-26-acid (see note 16). Possible alternatives to the 24-oxo group are an enol or epoxy group, all add 14 Da to the sterol structure.
5. Identification based on comparison with authentic standard.
6. Quantification based on [$^2H_6$]cholest-5-ene-3β,24(R/S)-diol internal standard.

7. Additional analysis of 18 individual control samples.
8. Cholest-4-ene-3β,6-diol and/or cholest-5-ene-3β,6-diol are decomposition products of 3β-hydroxycholestan-5,6-epoxide and cholestane-3β,5α,6β-triol. Identification based on comparison with 6β-hydroxycholest-4-en-3-one reference standard.
9. 7α-Hydroxy-3-oxocholest-4-en-26-oic acid dehydrates to a minor degree to 3-oxocholesta-4,6-dien-26-oic acid. Thus, the total 7α-hydroxy-3-oxocholest-4-en-26-oic acid corresponds to the sum of the two acids.
10. 3β,7α-Dihydroxycholest-5-en-26-oic acid dehydrates to a minor degree to 3β-hydroxycholesta-5,7-dien-26-oic acid. Thus, the total 3β,7α-dihydroxycholest-5-en-26-oic acid corresponds to the sum of the two acids.
11. Identification based on comparison with cholest-5-ene-3β,7α,25-triol and cholest-5-ene-3β,7β,25-triol reference standards.
12. The MS^n spectra suggest hydroxylation of the C-17 side-chain. 24-Hydroxy-3-oxocholesta-4,6-dien-26-oic acid is a likely dehydration product of 7α,24-dihydroxy-3-oxocholest-4-en-26-oic acid (see note 17).
13. The MS^n spectra suggest hydroxylation of the C-17 side-chain. 25-Hydroxy-3-oxocholesta-4,6-dien-26-oic acid is a likely dehydration product of 7α,25-dihydroxy-3-oxocholest-4-en-26-oic acid (see note 18).
14. The MS^n spectra suggest a 3β,22,25-trihydroxycholest-5-en-24-one or 3β,z-dihydroxycholest-5-en-26-oic acid structure, where z is a side-chain hydroxylation.
15. The MS^n spectra suggest dihydroxylation of the C-17 side-chain, possibly at C-24 or C-26 and C-25.
16. The MS^n spectra suggest a 24-oxo group. An alternative explanation is an enol or epoxy group, all add 14 Da to the sterol structure.
17. The MS^n spectra suggest a hydroxyl group on the C-17 side-chain, probably at C-24.
18. The MS^n spectra suggest a hydroxyl group on the C-17 side-chain, probably at C-25.
19. MS^n spectra of insufficient quality to define location of substituents.

Table S2. Oxysterols and Cholestenoic Acids in Human Plasma/Serum

Oxysterols and cholestenoic acids identified by LC-ESI-MS^n in plasma/serum following SPE and charge-tagging with GP-hydrazine. In the absence of authentic standards presumptive identifications based on exact mass, MS^n spectra and retention time are given. Control samples from 50 adults (blue†) and three children (black‡) were analysed. Data is given for seven adults showing clinically pure SPG5 plus two adults with complicated SPG5 (purple*) and three infants suffering from O7AHD (gold§). Data is also given for three healthy carriers, heterozygotes, with single mutations in *CYP7B1* (green•). Data is given four patients suffering from CTX (brown¶). Clinical data is given in Table S3.

After cholesterol oxidase and GP-tagging			Originating structure					
Mass	Formula	Sterol Systematic name	Sterol Systematic name (common name, abbreviation)	RT	RRT	AS	Mean concentration ng/mL±SEM	
506.3377	$C_{31}H_{44}N_3O_3^+$	3-Oxochol-4-en-24-oic acid 3-GP	3β-hydroxychol-5-en-24-oic acid (3βH-Δ^5-BA)	4.57	0.75	Y	0.83±0.14† 1.55±0.38‡ 6.06± 0.35• 22.28±4.53* 178.85±88.40§ ND¶	1, 2, 3
522.3326	$C_{31}H_{44}N_3O_4^+$	7α-Hydroxy-3-oxochol-4-en-24-oic acid 3-GP	7α-Hydroxy-3-oxochol-4-en-24-oic acid (7αH,3O-Δ^4-BA)	2.18	0.36	Y	1.17±0.23† 1.51±0.67‡ 1.41± 0.22• 1.24± 0.32* 11.38± 7.33§ ND¶	1, 2, 3
522.3326	$C_{31}H_{44}N_3O_4^+$	7α-Hydroxy-3-oxochol-4-en-24-oic acid 3-GP	3β,7α-Dihydroxychol-5-en-24-oic acid (3β,7α-diH-Δ^5-BA)	2.18	0.36	Y	1.52±0.34† 1.53±0.63‡ 1.26±0.02• 0.75± 0.42* 2.91± 2.38§ ND¶	1, 2, 3
532.3898	$C_{34}H_{50}N_3O_2^+$	Cholest-4-ene-3,24-dione 3-GP	Cholest-4-ene-3,24-dione	7.91	1.27	Y	0.36±0.03† ND‡ ND• ND* ND§ ND¶	1, 2, 3, 4
532.3898	$C_{34}H_{50}N_3O_2^+$	Cholest-4-ene-3,24-dione 3-GP	3β-Hydroxycholest-5-en-24-one	7.91	1.27	Y	0.24±0.06†	1,

			(24-Oxocholesterol, 24O-C)				ND‡ 0.65± 0.07• 0.37± 0.10* 38.74± 4.03§ 0.29± 0.23¶	2, 3, 4
534.3690	$C_{33}H_{48}N_3O_3^+$	7α-Hydroxy-26-nor-cholest-4-ene-3,**24**-dione 3-GP	7α-Hydroxy-26-nor-cholest-4-ene-3,**24**-dione	5.16	0.83	N	0.2±0.2† ND‡ 0.19± 0.11• 0.03±0.02* 5.10± 4.27§ ND¶	1, 2, 5, 6
534.4054	$C_{34}H_{52}N_3O_2^+$	24S-Hydroxycholest-4-en-3-one 3-GP	Cholest-5-ene-3β,24S-diol (24S-Hydroxycholesterol, 24S-HC)	7.60	1.24	Y	7.11±0.40† 12.67±0.26† 10.25± 1.95• 9.13± 1.94* 136.18± 43.06§ 10.11± 3.77¶	3, 7
534.4054	$C_{34}H_{52}N_3O_2^+$	25-Hydroxycholest-4-en-3-one 3-GP	Cholest-5-ene-3β,25-diol (25-Hydroxycholesterol, 25-HC)	7.91	1.29	Y	3.96±0.27† 6.04±0.97‡ 1.31± 0.05• 49.40± 11.38* 336.97± 86.56§ 3.60±1.23¶	2, 3, 7, 8
534.4054	$C_{34}H_{52}N_3O_2^+$	26-Hydroxycholest-4-en-3-one 3-GP	Cholest-5-ene-3β,26-diol (26-Hydroxycholesterol, 26-HC)	8.14	1.33	Y	18.99±0.85† 10.22±2.65‡ 38.54± 0.91• 97.75± 7.28* 1320.94±212.61§ ND¶	2, 3, 7
534.4054	$C_{34}H_{52}N_3O_2^+$	7β-Hydroxycholest-4-en-3-one 3-GP	7β-Hydroxycholest-4-en-3-one (7β-HCO)	9.84	1.60	Y	2.62±0.75† ND‡ ND• ND* ND§ ND¶	2, 3, 7, 9
534.4054	$C_{34}H_{52}N_3O_2^+$	7β-Hydroxycholest-4-en-3-one 3-GP	Cholest-5-ene-3β,7β-diol (7β-Hydroxycholesterol, 7β-HC)	9.84	1.60	Y	1.02±0.58† ND‡	2, 3,

							0.59± 0.12 12.77±12.52* 58.26±45.96§ 24.01±7.52¶	7, 9
534.4054	$C_{34}H_{52}N_3O_2^+$	3β-Hydroxycholest-5-en-7-one 7-GP	3β-Hydroxycholest-5-en-7-one (7-Oxocholesterol, 7O-C)	9.93	1.62	Y	4.98±2.25† ND‡ 2.42± 0.43 0.77±0.29* 25.00±19.60§ 34.35±24.15¶	1, 3, 9
534.4054	$C_{34}H_{52}N_3O_2^+$	7α-Hydroxycholest-4-en-3-one 3-GP	7α-Hydroxycholest-4-en-3-one (7α-HCO)	10.39	1.69	Y	2.43±0.37† ND‡ 4.03± 2.45• 3.19±0.79* 0.09±0.09§ 70.77±39.58¶	2, 3, 7, 9
534.4054	$C_{34}H_{52}N_3O_2^+$	7α-Hydroxycholest-4-en-3-one 3-GP	Cholest-5-ene-3β,7α-diol (7α-Hydroxycholesterol, 7α-HC)	10.39	1.69	Y	1.30±0.39† ND‡ 1.42± 0.31• 6.75±6.21* 36.39±30.67§ 78.25±51.06¶	2, 3, 7, 9
534.4054	$C_{34}H_{52}N_3O_2^+$	6-Hydroxycholest-4-en-3-one 3-GP	Cholest-4-ene-3β,6-diol or Cholest-5-ene-3β,6-diol (6-Hydroxycholesterol, 6-HC)	10.79	1.75	Y	1.96±0.50† ND‡ 0.30± 0.18• 0.22±0.19* ND§ 3.83±2.52¶	2, 3, 7, 9, 10
546.3690	$C_{34}H_{48}N_3O_3^+$	3-Oxocholesta-4,6-dien-26-oic acid 3-GP	3-Oxocholesta-4,6-dien-26-oic acid	7.52	1.23	Y	8.10±0.74† 2.57±1.56‡ 8.38± 1.24• 7.58±1.96* 16.56±9.53§ ND¶	1, 2, 3, 11
546.3690	$C_{34}H_{48}N_3O_3^+$	3-Oxocholesta-4,6-dien-26-oic acid 3-GP	3β-Hydroxycholesta-5,7-dien-26-oic acid	7.52	1.23	N	6.20±0.59† 2.56±0.60‡ 1.16± 0.57•	1, 2, 5,

							1.73±1.03* ND§ ND¶	12
548.3847	$C_{34}H_{50}N_3O_3^+$	3-Oxocholest-4-en-26-oic acid 3-GP	3β-Hydroxycholest-5-en-26-oic acid (3β-HCA)	7.84	1.28	Y	81.12±4.31† 37.21±7.77‡ 140.48± 22.60• 368.40±65.27* 2909.35±675.10§ ND¶	1, 2, 3
550.4003	$C_{34}H_{52}N_3O_3^+$	7α,25-Dihydroxycholest-4-en-3-one 3-GP	7α,25-Dihydroxycholest-4-en-3-one (7α,25-diHCO)	5.87	0.96	Y	1.10±0.32† 2.51±1.83‡ 0.88± 0.14• ND* ND§ 4.64±2.89¶	1, 2, 3
550.4003	$C_{34}H_{52}N_3O_3^+$	7α,26-Dihydroxycholest-4-en-3-one 3-GP	7α,26-Dihydroxycholest-4-en-3-one (7α,26-diHCO)	6.38	1.04	Y	5.10±0.56† 5.02±2.52‡ 3.55± 1.26• 1.32±0.26* 0.13±0.13§ ND¶	1, 2, 3
550.4003	$C_{34}H_{52}N_3O_3^+$	7α,26-Dihydroxycholest-4-en-3-one 3-GP	Cholest-5-ene-3β,7α,26-triol (7α,26-Dihydroxycholesterol, 7α,26-diHC)	6.38	1.04	Y	0.92±0.49† 1.27±0.26‡ 0.59± 0.11• 0.20±0.10* 0.57±0.57§ ND¶	1, 2, 3
550.4003	$C_{34}H_{52}N_3O_3^+$	7α,12α-Dihydroxycholest-4-en-3-one 3-GP	7α,12α-Dihydroxycholest-4-en-3-one (7α,12α-diHCO)	9.23	1.51	Y	ND† ND‡ 0.05± 0.05• ND* NDS§ 381.62±250.33¶	1, 2, 3,
550.4003	$C_{34}H_{52}N_3O_3^+$	7α,12α-Dihydroxycholest-4-en-3-one 3-GP	Cholest-5-ene-3β,7α,12α-triol (7α,12α-Dihydroxycholesterol, 7α,12α-diHC)	9.23	1.51	Y	ND† ND‡ 0.05±0.03• ND*	1, 2, 3,

							ND§ 95.60±76.01¶	
562.3639	$C_{34}H_{48}N_3O_4^+$	**24**-Hydroxy-3-oxocholesta-4,6-dien-26-oic acid 3-GP	**24**-Hydroxy-3-oxocholesta-4,6-dien-26-oic acid	4.39	0.71	N	0.2±0.2† 0.2±0.2‡ ND• 0.29±0.17* ND§ ND¶	1, 2, 5, 13
564.3796	$C_{34}H_{50}N_3O_4^+$	7β-Hydroxy-3-oxocholest-4-en-26-oic acid 3-GP	3β,7β-Dihydroxycholest-5-en-26-oic acid (3β,7β-diHCA)	4.45	0.73	Y	1.67±0.32† 3.11±1.00‡ 3.31± 1.25• 2.74±0.58* 8.83±4.42§ ND¶	1, 2, 3
564.3796	$C_{34}H_{50}N_3O_4^+$	**22**,**25**-Dihydroxycholest-4-en-3,**24**-dione 3-GP	3β,**22**,**25**-Trihydroxycholest-5-en-**24**-one	5.44	0.88	N	5.37±0.64† 4.74±1.59‡ 6.36± 1.58• 15.70±3.30* 29.77±4.06§ 7.10±1.29¶	1, 2, 5, 14
564.3796	$C_{34}H_{50}N_3O_4^+$	7α-Hydroxy-3-oxocholest-4-en-26-oic acid 3-GP	7α-Hydroxy-3-oxocholest-4-en-26-oic acid (7αH,3O-CA)	6.11	1.00	Y	65.27±6.22† 48.32±16.97‡ 59.53± 6.41• 33.95±5.81* 29.79±14.82§ ND¶	1, 2, 3, 11
564.3796	$C_{34}H_{50}N_3O_4^+$	7α-Hydroxy-3-oxocholest-4-en-26-oic acid 3-GP	3β,7α-Dihydroxycholest-5-en-26-oic acid (3β,7α-diHCA)	6.11	1.00	Y	39.40±3.95† 28.83±8.40‡ 18.76± 5.14• 5.21±3.09* 1.16±1.16§ ND¶	1, 2, 3, 12
566.3952	$C_{34}H_{52}N_3O_4^+$	7α,**24**(or**26**),**25**-Trihydroxycholest-4-en-3-one 3-GP	7α,**24**(or**26**),**25**-Trihydroxycholest-4-en-3-one	2.84	0.46	N	0.65±0.11† 3.38±2.36‡ NM• ND* 1.60±0.80§	1, 2, 5, 15

							ND¶	
580.3745	$C_{34}H_{50}N_3O_5^+$	7α,**24**-Dihydroxy-3-oxocholest-4-en-26-oic acid 3-GP	7α,**24**-Dihydroxy-3-oxocholest-4-en-26-oic acid	2.89	0.47	N	0.2±0.2† 0.56±0.44‡ 0.99± 0.09• ND* ND§ ND¶	1, 2, 5, 16

RT = Retention time/min; RRT = Retention time relative to 7α-hydroxy-3-oxocholest-4-en-26-oic acid; AS = Authentic standard, Y = Yes, N = No; SEM = Standard error of the mean; ND = Not detected; NM = Not measured. In some cases the exact location of the side-chain oxo or hydroxy groups is equivocal in which case the most likely location is shown in **bold**. Some of the data for children suffering from O7AHD is reported in (10).

1. Quantitative estimate based on [$^2H_6$]cholest-5-ene-3β,24(R/S)-diol internal standard.
2. Quantitative measurements based on GP-tagged 3-oxo-4-ene compounds giving similar ESI-MS response (9).
3. Identification based on comparison with authentic standard.
4. 24S,25-Epoxycholesterol can isomerise to 3β-hydroxycholest-5-en-24-one during sample preparation.
5. Identification based on exact mass and MS^n spectra.
6. 26-Nor-sterol is a likely decomposition product of a 24-oxo-26-acid. Alternatives to the oxo group are an enol or epoxy group, all add 14 Da to the sterol structure.
7. Quantification based on [$^2H_6$]cholest-5-ene-3β,24(R/S)-diol internal standard.
8. There is some tailing of the 24S-hydroxycholesterol peak into the 25-hydroxycholesterol peak, thus, values for 25-hydroxycholesterol are likely to be overestimated particularly when concentrations of 24S-hydroxycholesterol greatly exceed those of 25-hydroxycholesterol.
9. May be underestimation of levels of late eluting oxysterols.
10. Cholest-4-ene-3β,6-diol and/or cholest-5-ene-3β,6-diol are decomposition products of 3β-hydroxycholestan-5,6-epoxide and cholestane-3β,5α,6β-triol. Identification based on comparison with 6β-hydroxycholest-4-en-3-one reference standard.
11. 7α-Hydroxy-3-oxocholest-4-en-26-oic acid dehydrates to a minor degree to 3-oxocholesta-4,6-dien-26-oic acid. Thus, the total 7α-hydroxy-3-oxocholest-4-en-26-oic acid corresponds to the sum of the two acids.
12. 3β,7α-Dihydroxycholest-5-en-26-oic acid dehydrates to a minor degree to 3β-hydroxycholesta-5,7-dien-26-oic acid. Thus, the total 3β,7α-dihydroxycholest-5-en-26-oic acid corresponds to the sum of the two acids.
13. The MS^n spectra suggest hydroxylation of the C-17 side-chain. 24-Hydroxy-3-oxocholesta-4,6-dien-26-oic acid is a likely dehydration product of 7α,24-dihydroxy-3-oxocholest-4-en-26-oic acid (see note 16).
14. The MS^n spectra suggest a 3β,22,25-trihydroxycholest-5-en-24-one or 3β,z-dihydroxycholest-5-en-26-oic acid structure, where z is a side-chain hydroxylation.
15. The MS^n spectra suggest dihydroxylation of the C-17 side-chain, possibly at C-24 or C-26 and C-25.
16. The MS^n spectra suggest a hydroxy group on the C-17 side-chain, probably at C-24.

Table S3. Mutations in SPG5, O7AHD and CTX Patients Studied

Sample code	Mutation	Reference	Family	Comment
				HSP
P4505 II-1 (sister)	Compound heterozygous *CYP7B1* c.260G>T/p.G87V c.889A>G/p.T297A	Arnoldi et al (11)	P4505	Pure HSP (serum analysed)
P4505 II-2 (sister)	Compound heterozygous *CYP7B1* c.260G>T/p.G87V c.889A>G/p.T297A	Arnoldi et al (11)	P4505	Pure HSP (serum analysed)
P52405	Homozygous *CYP7B1* c.1328G>C/p.G443A	Arnoldi et al (11)	P52405	Complicated HSP (serum analysed)
Patient 2 (female)	Homozygous *CYP7B1* c.825T>A/p.Y275X	Schűle et al (12)		Complicated HSP (serum and CSF analysed)
AC (male)	Homozygous *CYP7B1* c.889A>G/p.T297A	Present work		Pure HSP (plasma analysed)
P II-1 (male)	Homozygous *CYP7B1* c.806delA/p.D269VfsX282	Criscuolo et al (13)	Family P	Pure HSP (plasma analysed)
S II-3 (female)	Homozygous *CYP7B1* c.806delA/p.D269VfsX282	Criscuolo et al (13)	Family S	Pure HSP (plasma analysed)
Si II-1 (male)	Homozygous *CYP7B1* c.1362insT/p.A453CfsX470	Criscuolo et al (13)	Family Si	Pure HSP (plasma analysed)
G1 (male)	Compound heterozygous *CYP7B1* c.250delC/p.L84FfsX6 c.266A>C/p.Y89S	Present work	Family G	Pure HSP (serum and CSF analysed)
22332	Homozygous *CYP7B1* c.1456C>T/p.R486C	Present work		(CSF analysed)
				O7AHD

JP (Infant male)	Homozygous *CYP7B1* c.538C>T/p.R112X	Ueki et al (14)		O7AHD on treatment with UDCA (plasma analysed)
LT (Infant female)	Compound heterozygous *CYP7B1* c.538C>T/p.R112X c.1453C>T/p.R417C	Mizuochi et al (15)		O7AHD on treatment with UDCA (plasma analysed)
JI (Infant male)	Homozygous *CYP7B1* c.1249C>T/p.R417C	Dai et al (10) Chong et al (16)		O7AHD on treatment with UDCA (plasma analysed)
				Heterozygote Carriers (healthy) Controls
G2(male)	Heterozygous *CYP7B1* c.250delC/p.L84FfsX6	Present work	Family G	Father of G1, unaffected (serum and CSF analysed)
G3 (female)	Heterozygous *CYP7B1* c.266A>C/p.Y89S	Present work	Family G	Mother of G1, unaffected (serum and CSF analysed)
G4 (male)	Heterozygous *CYP7B1* c.266A>C/p.Y89S	Present work	Family G	Brother of G1, unaffected (serum analysed)
				CTX
8876 Adult (female)	Homozygous *CYP27A1* c.526delG/p.T175fsX5	Present work	Family 887	CTX On treatment with CDCA and simvastatin (plasma analysed)
8875 Adult (male)	Homozygous *CYP27A1* c.526delG/p.T175fsX5	Present work	Family 887	CTX On treatment with CDCA and simvastatin (plasma analysed)
8577 Child (male)	Homozygous *CYP27A1* c.1184+1G>A	Bourkiza et al (17)		CTX Not on treatment (plasma analysed)
S2 Child (male)	Homozygous *CYP27A1* IVS 6+1G>A	Present work		CTX Not on treatment. Diagnosis based on clinical and biochemical grounds. Mutation analysis performed on affected brother (plasma analysed)

Two of the CTX samples were from siblings born to consanguineous, second cousin parents. The older sibling (8876), had global developmental delay with significant motor and speech delay, brisk reflexes and tight Achilles tendons. Nerve conduction studies were suggestive of hereditary motor sensory neuropathy type 2. She developed bilateral cataracts as a teenager and was diagnosed at age 20. She was ataxic with poor finger-nose coordination. Her brain MRI showed high signal bilaterally in the dentate nucleus and posterior pallidus on T2 weighted images. The brother (8875) was diagnosed at age 18, he had brisk reflexes and poor finger-nose coordination, but no other findings. His brain MRI showed high signal in the deep white matter of both occipital lobes on T2 weighted sequences. Both siblings were homozygous for a mutation c.526delG in *CYP27A1* leading to a frameshift and the introduction of a premature stop codon. At the time of sampling both siblings were on treatment with CDCA and simvastatin. A third CTX sample was from a 15 year old boy (8577) with bilateral pulverulent cataracts, brisk bilateral reflexes, cerebellar ataxia, broad gait and learning difficulties (17). He was from consanguineous parents and homozygous for the intron 6 c.1184+1G>A mutation in *CYP27A1* leading to aberrant splicing. He was not on treatment at the time of sampling. A fourth CTX patient (S2) was aged nine and not on treatment. He presented with delayed acquisition of language and dysarthria. He has recurrent bouts of diarrhoea. He does not have cataracts or spasticity or ataxia. The diagnosis of CTX was made on clinical and biochemical grounds i.e. high plasma cholestanol (5α-cholestan-3β-ol). His brother who also suffers from CTX is homozygous for the IVS 6+1G>A mutation in *CYP27A1*.

Two SPG5 samples were from patients P4505 II-1 and P4505 II-2 whose clinical phenotype was pure HSP and was reported earlier (11). The patients were siblings, the younger sister (P4505 II-2) showed a severe phenotype, early age at onset and long disease history, while the older sister (P4505 II-1) manifest a very mild disease with just lower limb brisk reflexes and very mild spasticity. The two sisters were heterozygous for the exon 3 c.260G>T/p.G87V and exon 4 c.889A>G/p.T297A mutations in *CYP7B1*. A third sample was from patient P52405 with complicated HSP also reported earlier (11). This patient was homozygous for the exon 6 c.1328G>C/p.G443A missence mutation in *CYP7B1*. The patient is wheelchair bound after 23 years of disease duration. A second patient with complicated HSP was patient 2 in Schüle et al (12). This patient, a 44-year-old female, was 18 years old at onset. At age 41 she presented with severe dorsal column affection and optic atrophy in addition to spastic paraparesis. She also suffers from intermittent diarrhoea. She is

homozygous for the nonsense mutation c.825T>A/p.Y275X. Five further samples were from patients with the pure HSP phenotype, three of which were reported earlier by Criscuolo et al (13). The clinical phenotype of the patients was progressive spastic paraplegia with variable bladder and sensory involvement. Further clinical data is presented in Table 1 of reference (13). Patient AC was homozygous for the mutation in exon 4 c.889A>G/p.T297A. Patients P II-1 and S II-3 were from different families but were homozygous for the same truncating mutation in exon 3 c.806delA/p.D269VfsX282. The mutation c.806delA creates a frameshift at amino acid 269, a premature stop codon at amino acid 282, and a truncated protein. The fourth patient Si II-1 was homozygous for the truncating mutation in exon 6 c.1362insT/p.A453CfsX470. The mutation c.1362insT leads to a frameshift at amino acid 453, the introduction of a premature stop codon at position 470 and a truncated protein. Sample G1 is a 16 year-old male from a nonconsanguineous family of Greek origin (brother G4, mother G3, father G2). He suffers from pure HSP that started with spastic gait disturbance at the age of 2. Clinical presentation at the age of 16 encompasses spastic paraparesis with moderate-to-severe lower limb (LL) spasticity, bilateral Babinski and mild-to-moderate proximal LL weakness (pyramidal affection), and mild LL sensory ataxia with bilateral distal decrease in vibration and joint-position sensibility (dorsal column affection). He did not have cognitive or detrusor-sphincter disturbance. MRI of brain and spinal cord were normal with no hyperintensities. There were no signs of peripheral neuropathy in ENMG. He is compound heterozygote for a frameshift mutation (c.250delC/p.L84FfsX6) and a missense mutation(c.266A>C/p.Y89S). The patient can still ambulate without walking aids. CSF was analysed from a final patient 22332 with the homozygous mutation c.1456C>T/p.R486C in *CYP7B1*.

Two patients from East Asia with neonatal cholestatic liver disease were a male (JP), homozygous for the mutation c.538C>T/p.R112X leading to a stop codon at residue 112 in *CYP7B1* (14), and a female (LT) heterozygous for the mutations c.538C>T/p.R112X and c.1453C>T/p.R417C leading to an arginine to cystine substitution at residue 417 in CYP7B1 (15). Both patients were treated with ursodeoxycholic acid (3α,7β-dihydroxy-5β-cholan-24-oic acid, UDCA) at the time of sampling. A third patient (JI), presented at 3 weeks with hyperbilirubinaemia, and at three months developed coagulopathy, hypoalbuminaemia, irritability and episodic hypoglycaemia (16). He was on UDCA treatment at the time of sampling. Diagnosis was made on clinical and biochemical grounds.

The patient was homozygous for the missense mutation c.1249C>T/p.R417C in *CYP7B1* which changes a highly conserved arginine to a cystine residue at 417 in the protein.

Table S4. Sterols in the Cholestenoic Acid Biosynthetic Pathways in *Cyp7b1-/- and Cyp27a1-/-* Mouse Brain and Plasma
Cholestenoic acids identified by LC-ESI-MS^n following SPE and charge-tagging with GP-hydrazine.

Sterol Systematic name (abbreviation)	Mouse age (months)	Mean concentration in brain (ng/mg±SD)		Mean concentration in plasma (ng/mL±SD)		
		WT	*Cyp7b1-/-*	WT	*Cyp7b1-/-*	Note
Cholest-5-ene-3β,26-diol (26-HC)	13 23	0.25±0.03 1.09±0.28	4.34±0.54*** 5.45±0.30***	5.80± 1.62 4.00± 0.88	23.80± 4.61*** 16.93± 4.05***	1,2,3
Cholest-5-ene-3β,7α,26-triol (7α,26-diHC) + 7α,26-dihydroxycholest-4-en-3-one (7α,26-diHCO)	13 23	0.02±0.01 0.03±0.01	0.01± 0.00 0.05± 0.01	1.10± 0.44 1.30± 0.49	0.64± 0.14 0.69± 0.43	1,2,3
3β-Hydroxycholest-5-en-26-oic acid (3β-HCA)	13 23	0.01±0.00 0.01±0.00	0.12±0.02*** 0.15±0.01***	1.97±0.72 1.75±0.50	7.32±1.50*** 6.69±2.64**	1,2,3
7α-Hydroxy-3-oxocholest-4-en-26-oic acid (7αH,3O-CA)	13 23	ND ND	ND ND	25.89±10.91 25.19±9.44	14.21±3.76 20.73±1.77	1,2,3
3β,7α-Dihydroxycholest-5-en-26-oic acid (3β,7α-diHCA)	13 23	ND ND	ND ND	ND ND	ND ND	1,2,3
		WT	*Cyp27a1-/-*	WT	*Cyp27a1-/-*	
Cholest-5-ene-3β,26-diol (26-HC)	3	0.09±0.01	0.01± 0.00***	9.58±1.70	ND***	2,3,4
Cholest-5-ene-3β,7α,26-triol (7α,26-diHC)	3	ND	ND	0.04± 0.02	ND*	2,3,4
7α,26-dihydroxycholest-4-en-3-one (7α,26-diHCO)	3	ND	ND	0.10± 0.03	3.76± 0.44	2,3,4 ,5
3β-Hydroxycholest-5-en-26-oic acid (3β-HCA)	3	ND ND	ND ND	3.56±1.22	ND**	2,3,4
7α-Hydroxy-3-oxocholest-4-en-26-oic acid (7αH,3O-CA)	3	ND ND	ND ND	28.96±7.22	5.23±1.07**	2,3,4 ,5
3β,7α-Dihydroxycholest-5-en-26-oic acid (3β,7α-diHCA)	3	ND ND	ND ND	ND ND	ND ND	2,3,4

1. Wild type (WT) and *Cyp 7b1-/-* mouse plasma (13 months, n = 5; 23 months, n = 4) and brain (13 months, n = 3; 23 months, n = 4).
2. Data are means ± SD, *, $P < 0.05$; **, $P < 0.01$; ***, $P < 0.001$, by Student's *t*-test, compared to same age WT.
3. Quantification was by stable isotope dilution mass spectrometry using deuterated 24(R/S)-hydroxycholesterol as the internal standard.
4. Samples were from wild type (WT) and *Cyp27a1-/-* mice at 3 months, n = 3.
5. 7α,26-diHCO and 7αH,3O-CA in *Cyp27a1-/-* mouse plasma are probably the 25S-epimers formed by an alternative sterol hydroxylase to CYP27A1.

References

(1) Zhang J, Akwa Y, el-Etr M, Baulieu EE, Sjövall J. Metabolism of 27-, 25- and 24-hydroxycholesterol in rat glial cells and neurons. *Biochem J* 1997; 322 (Pt 1):175-84.

(2) Karu K, Turton J, Wang Y, Griffiths WJ. Nano-liquid chromatography-tandem mass spectrometry analysis of oxysterols in brain: monitoring of cholesterol autoxidation. *Chem Phys Lipids* 2011; 164(6):411-24.

(3) Meljon A, Theofilopoulos S, Shackleton CH *et al.* Analysis of bioactive oxysterols in newborn mouse brain by LC/MS. *J Lipid Res* 2012; 53(11):2469-83.

(4) Shafaati M, Marutle A, Pettersson H *et al.* Marked accumulation of 27-hydroxycholesterol in the brains of Alzheimer's patients with the Swedish APP 670/671 mutation. *J Lipid Res* 2011; 52(5):1004-10.

(5) Wang Y, Sousa KM, Bodin K *et al.* Targeted lipidomic analysis of oxysterols in the embryonic central nervous system. *Mol Biosyst* 2009; 5(5):529-41.

(6) Griffiths WJ, Wang Y. Analysis of oxysterol metabolomes. *Biochim Biophys Acta* 2011; 1811(11):784-99.

(7) Ogundare M, Theofilopoulos S, Lockhart A *et al.* Cerebrospinal fluid steroidomics: are bioactive bile acids present in brain? *J Biol Chem* 2010; 285(7):4666-79.

(8) Fahy E, Subramaniam S, Brown HA *et al.* A comprehensive classification system for lipids. *J Lipid Res* 2005; 46(5):839-61.

(9) Karu K, Hornshaw M, Woffendin G *et al.* Liquid chromatography-mass spectrometry utilizing multi-stage fragmentation for the identification of oxysterols. *J Lipid Res* 2007; 48(4):976-87.

(10) Dai D, Mills PB, Footitt E *et al.* Liver disease in infancy caused by oxysterol 7alpha-hydroxylase deficiency: successful treatment with chenodeoxycholic acid. *J Inherit Metab Dis* 2014.

(11) Arnoldi A, Crimella C, Tenderini E *et al.* Clinical phenotype variability in patients with hereditary spastic paraplegia type 5 associated with CYP7B1 mutations. *Clin Genet* 2012; 81(2):150-7.

(12) Schüle R, Siddique T, Deng HX *et al.* Marked accumulation of 27-hydroxycholesterol in SPG5 patients with hereditary spastic paresis. *J Lipid Res* 2010; 51(4):819-23.

(13) Criscuolo C, Filla A, Coppola G *et al.* Two novel CYP7B1 mutations in Italian families with SPG5: a clinical and genetic study. *J Neurol* 2009; 256(8):1252-7.

(14) Ueki I, Kimura A, Nishiyori A *et al.* Neonatal cholestatic liver disease in an Asian patient with a homozygous mutation in the oxysterol 7alpha-hydroxylase gene. *J Pediatr Gastroenterol Nutr* 2008; 46(4):465-9.

(15) Mizuochi T, Kimura A, Suzuki M *et al.* Successful heterozygous living donor liver transplantation for an oxysterol 7alpha-hydroxylase deficiency in a Japanese patient. *Liver Transpl* 2011; 17(9):1059-65.

(16) Chong CP, Mills PB, McClean P, Clayton PT. Response to chenodeoxycholic acid therapy in an infant with oxysterol 7alpha-hydroxylase deficiency. *J Inherit Metab Dis* 2010; 33(Suppl 1):S-382.

(17) Bourkiza R, Joyce S, Patel H *et al.* Cerebrotendinous xanthomatosis (CTX): an association of pulverulent cataracts and pseudo-dominant developmental delay in a family with a splice site mutation in CYP27A1--a case report. *Ophthalmic Genet* 2010; 31(2):73-6.